Available online at www.sciencedirect.com
SCIENCE DIRECT®
Journal of Magnetic Resonance 180 (2006) 178–185
JMR Journal of Magnetic Resonance
www.elsevier.com/locate/jmr

Distance between a native cofactor and a spin label in the reaction centre of *Rhodobacter sphaeroides* by a two-frequency pulsed electron paramagnetic resonance method and molecular dynamics simulations

Igor V. Borovykh [a,b], Stefano Ceola [c,1], Prasad Gajula [a], Peter Gast [b]
Heinz-Jürgen Steinhoff [a], Martina Huber [c,*]

[a] *Fachbereich Physik, Universität Osnabrück, P.O. Box, 49069 Osnabrueck, Germany*
[b] *Department of Biophysics, Huygens Laboratory, Leiden University, The Netherlands*
[c] *Department of Molecular Physics, Huygens Laboratory, Leiden University, P.O. Box 9504, 2300 RA Leiden, The Netherlands*

Received 17 November 2005; revised 31 December 2005

Abstract

The distance between the paramagnetic state of a native cofactor and a spin label is measured in the photosynthetic reaction centre from the bacterium *Rhodobacter sphaeroides* R26. A two-frequency pulsed electron paramagnetic resonance method [double-electron–electron spin resonance (DEER)] is used. A distance of 3.05 nm between the semiquinone anion state of the primary acceptor (Q_A) and the spin label at the native cysteine at position 156 in the H-subunit is found. Molecular-dynamics (MD) simulations are performed to interpret the distance. A 6 ns run comprising the entire RC protein yields a distance distribution that is close to the experimental one. The average distance found by the MD simulation is smaller than the distance obtained by DEER by at least 0.2 nm. To better represent the experiments performed at low temperature (60 K), a MD method to mimic the freezing-in of the room-temperature conformations is introduced. Both MD methods yield similar distances, but the second method has a trend towards a wider distance distribution.

Keywords: Double-electron–electron resonance; Molecular-dynamics simulations; Spin-label EPR; Distance determination; Reaction centre *Rhodobacter sphaeroides*

1. Introduction

Methods for distance determination in biological systems are sought to obtain structure information in cases where the more conventional methods, such as X-ray crystallography, cannot be applied. This is often the case for membrane proteins, in particular when investigating conformational changes related to electron-transfer events. Given the large influence of the donor–acceptor distance on the electron-transfer rates, and the importance of conformational changes in the regulation of these processes, structural information is of particular relevance. The reaction centre (RC) of bacterial photosynthesis is one of the paradigmatic electron-transfer membrane proteins. Early on, differences in electron-transfer rates depending on the history of the sample had been found, and structural changes were implicated as one possible origin for that [1]. Information about structural changes upon electron-transfer events in this system is available from X-ray crystallography. The neutral state was compared to the final charge separated state, where the primary electron donor (D) is oxidized (D^+) and the final, secondary quinone (Q_B) was reduced (Q_B^-) [2]. Besides major changes around

* Corresponding author. Fax: +31 715275819.
E-mail address: mhuber@molphys.leidenuniv.nl (M. Huber).
[1] Present address: Department of Chemical Science, University of Padova Via Marzolo 1, 35131 PD, Italy.

1090-7807/$ - see front matter © 2006 Elsevier Inc. All rights reserved.
doi:10.1016/j.jmr.2006.02.008

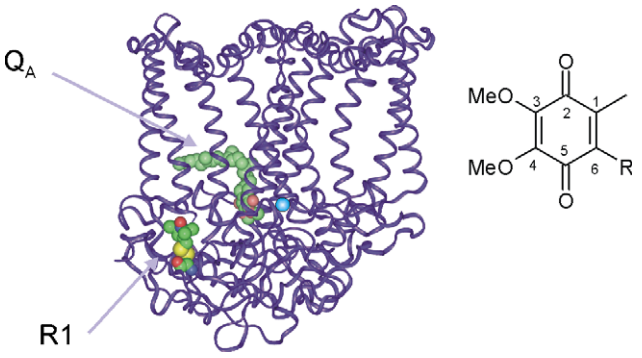

Fig. 1. Structure of the reaction centre with Q_A, the Fe-(II) ion (blue dot), and the spin-labelled cysteine (R1) highlighted (left). Numbering scheme of ubiquinone, R: isoprenoid C_{10} chain (right).

the Q_B binding site, also small changes of structure in other regions of the protein were detected.

Here we explore the possibility to address such questions by a pulsed, two-frequency EPR method double electron electron spin resonance (DEER) in combination with molecular-dynamics (MD) simulations on a reaction centre (RC) of the bacterium *Rhodobacter sphaeriodes* R26. The distance between a natural cofactor, the primary quinone acceptor (Q_A), and a spin label is investigated (Fig. 1). To do so, the quinone is reduced to the semiquinone anion radical state Q_A^-, and the spin label is attached to the native cysteine at position 156 in the H-subunit (H156) [3,25].

Previously, in other proteins, distances between two spin labels, often introduced by site-directed mutagenesis have been measured. Relating the distances between two spin labels to the structure of the protein is hampered by the unknown orientation of the 0.5 nm long linker joining the spin label to the protein backbone [4]. Combining a native cofactor that is fixed in the protein with a spin label should reduce that uncertainty without sacrificing the flexibility the spin-label approach offers with respect to the region of the protein to be probed.

Molecular-dynamics (MD) simulations are performed to analyse the spin-label linker conformation in order to compare the distance obtained by DEER with the X-ray structure. As the experimental data are obtained on a frozen sample, an MD approach is proposed to simulate the freezing-in of the room-temperature conformations.

We show that by DEER, the distance between the spin label at position H156 and the native cofactor Q_A^- can be determined with high precision. The MD simulations with a length of 6 ns yield a good agreement with the width and the shape of the distance distribution obtained by DEER, but result in a smaller distance than experimentally observed. The origin of this difference is discussed.

2. Results

The EPR experiments were performed on spin labelled RC's, in which the native Fe(II)-ion ($S = 2$), which forms a magnetically coupled spin pair with the Q_A^- radical, was replaced with the diamagnetic Zn(II) (SL-ZnRCs). The semiquinone-anion radical of Q_A (Q_A^-) was generated by photoreduction (see Section 4). In Fig. 2, the ese-detected EPR spectrum of the sample is shown. The two paramagnetic centres, i.e. the nitroxide and the Q_A^-, give rise to two signals. The EPR signal of Q_A^- (dashed line) contributes to the intensity in the central part of the spectrum and the spin label has the typical nitroxide powder spectrum (dotted line). The amount of Q_A^- formed by illumination is determined from the frozen solution cw-EPR spectrum of the sample. Simulations accounting for the superposition of the spin label and the Q_A^- EPR signal reveal a yield of 0.95 ± 0.1 of Q_A^- relative to the spin-label signal. As the spin-labelling efficiency is determined to be 0.9 ± 0.2 for the SL-ZnRC sample, an almost 1:1 ratio of spin label and Q_A^- signal indicates that Q_A^- is generated with high efficiency, and that almost all spin-labelled RCs contain Q_A^-.

Fig. 3A shows the DEER time traces of the light and the dark samples, performed under the same experimental conditions. Whereas the time trace of the dark sample reveals no distinct modulation, the trace of the light sample shows a pronounced modulation, which amounts to 5% modulation depth. As only intramolecular spin–spin interactions give rise to modulation in the DEER experiment, the modulation reveals the interaction between the two paramagnetic centres, the spin label and the Q_A^-. By Fourier transformation, the frequency of the modulation, which is related to the distance, can be obtained (Fig. 3B). It shows a peak at 2 MHz, revealing a distance of 3.0 nm. Time traces were analysed according to Jeschke et al. [5–7]. Simulations using Gaussian distance distributions yield the distances shown in Fig. 3C: A major component at 3.05 nm with a width (full-width at half-height) of 0.24 nm (Table 1) and a minor component (max. 20% of the spin pairs) with a distance of 4.5 nm and a width

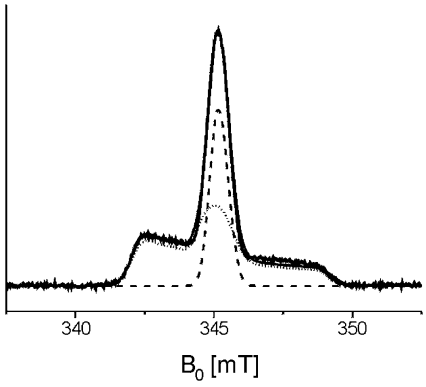

Fig. 2. Electron-spin-echo detected EPR signal (absorption mode) of the SL-ZnRC after illumination. Experimental conditions: temperature, $T = 15$ K; pulses, $p_{\pi/2} = 16$ ns, $p_{\pi} = 32$ ns; $\tau = 150$ ns; repetition time, 2 s. As the repetition time is small with respect to the longitudinal relaxation time (T_1) of Q_A^-, but not of the nitroxide, the relative intensity of the Q_A^- signal compared with the nitroxide signal is smaller than in cw-EPR (see text). Simulations: dashed line, spectrum of Q_A^-; dotted line, nitroxide spin label; thin solid line, superposition.

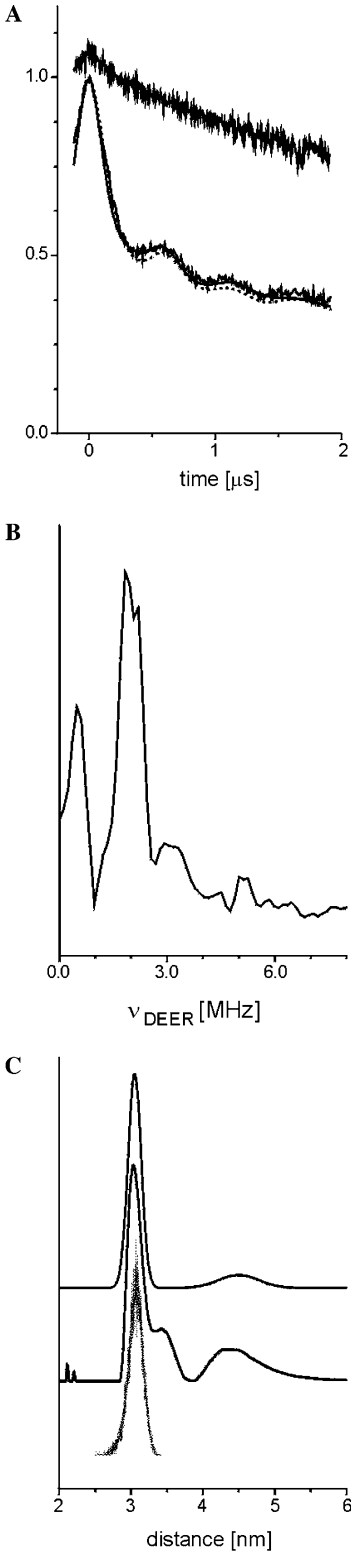

Fig. 3. Results of DEER experiments on SL-ZnRCs: (A) DEER time traces of light (bottom) and dark sample (top); thin solid line, fit using Gaussian distance distribution; dotted line, Tikhonov regularization (see text). (B) Fourier transform of DEER time trace of light sample. (C) Distance distributions: Gaussian distribution (top), result of Tikhonov regularization (centre); distance distribution from MD simulation shifted by +0.28 nm to facilitate comparison (bottom).

Table 1
Distances obtained from DEER experiments and MD calculations

	Distance (nm)	Width[a] (nm)
DEER	3.05(5)	0.24(2)
MD	2.80(5)	0.17(5)
MD[b]	2.80(5)	0.25(5)

[a] Full width at half height.
[b] From energy-minimized structures from MD run. Gaussian fit of histogram shown in Fig. 4B.

of 0.8 nm. The origin of the minor component is not clear at present. For the major component, the error to determine the centre of the distribution is 0.05 nm. Fitting the data with an arbitrary distance distribution (model-free approach), as proposed in [8,9], results in a slightly different distance distribution (Fig. 3C). For the main peak at 3.05 nm, the distribution is close to Gaussian with an additional contribution of lower amplitude centered around 3.45 nm. Comparing the fits to the data (Fig. 3A), the model-free approach (dotted line, Fig. 3A) only slightly improves the fit to the data compared to the Gaussian distance distribution (thin solid line, Fig. 3A), suggesting that a Gaussian distribution describes the data sufficiently well. The absence of modulation in the dark sample confirms that the distance of 3.05 nm is due to the interaction of the spin label with the light-induced Q_A^-.

The results of the MD simulations are shown in Fig. 4A, where the distances between the geometrical centre of the N- and O-atoms of the nitroxide and the O5 atom of the Q_A are depicted. The trajectory is flat, revealing that the overall structure is well equilibrated during the trajectory. The distribution of distances for all structures of the MD run is shown in Fig. 4B. For comparison with the experimental data, the distribution is fitted to a Gaussian lineshape with the parameters given in Table 1. In Table 2, the distances from the spin label to all Q_A-ring atoms are listed for one structure at the centre of the distribution. It reveals that the orientation of Q_A is such that the distance from the nitroxide to O5 is larger than that to the remaining ring atoms of the Q_A. To illustrate the conformations of the spin label during the MD run, the position of the nitroxide group relative to Q_A is shown in Fig. 5 for 15,000 frames of the trajectory.

Energy minimization was performed for 30 structures, chosen at random time points of the MD run. The distribution of NO-O5 distances obtained from these structures is shown as a histogram superimposed on the distance distribution in Fig. 4B. The distance at which the maximum of the distance distribution is located is similar in the two cases, but the histogram is flatter at the top, an indication that the energy-minimized structures could have a broader distance distribution. Fitting the histogram to a Gaussian results in the parameters given in Table 1.

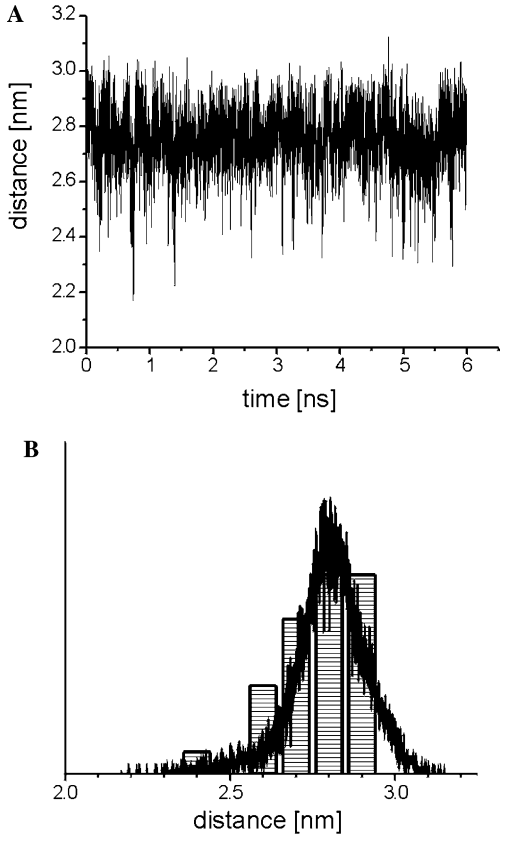

Fig. 4. Distance between O5 of Q_A and the centre of the N–O bond of the spin label for all frames of the MD run (A). (B) Distance distribution of (A) with histogram of results of energy minimization on 30 structures (see text).

Table 2
Distance from Q_A ring atoms to the spin label NO group for a typical structure of the MD run

Q_A-ring atom	Distance (nm)
C1	2.61
C2	2.54
C3	2.57
C4	2.67
C5	2.74
C6	2.69
C1M	2.55
O2	2.44
O5	2.83

3. Discussion

We explore, whether the changes in protein conformation related to electron-transfer events could, in principle, be detected by measuring the distance between a native cofactor and a spin label in an electron-transfer membrane protein. To measure this distance, the DEER technique is employed. The modulation observed in the DEER time traces (Fig. 3A) is evidence for the interaction of the cofactor (Q_A^-) and the spin label at H156. The frequency of the modulation corresponds to a distance of approximately

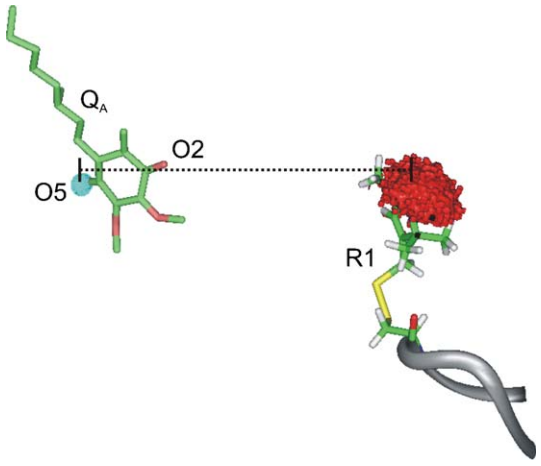

Fig. 5. Conformational space covered by the nitroxide group (shown in red for 15,000 frames of the trajectory) of the spin-label side-chain (R1) at position H156 and relative orientation of Q_A. In grey, section of the backbone of the H-subunit. The position of O5 of Q_A is shown in blue; separation between Q_A and R1 not drawn to scale.

3 nm. This distance is too large to result in significant line broadening of the cw-EPR spectra, emphasizing the need to employ the DEER technique.

Further analysis shows that the distance distribution has a Gaussian shape, the centre of which is at 3.05 nm and can be determined with a precision of 0.05 nm. The width of the distance distribution is 0.24 nm. A small additional component at a distance larger than 4 nm is found, the origin of which is unclear at present.

To obtain more detailed structural information from the DEER experiment, it has to be taken into account that the dipolar interaction is proportional to $1/r^3$ with r, the distance between the centres of spin density on the two paramagnetic partners. Thus, the distribution of spin density over the semiquinone ring of the Q_A^- and over the nitroxide group of the spin label needs to be known.

The spin density on Q_A^- is distributed over the entire quinone ring, with the majority at the ring C–O-groups. It is known that the spin-density distribution is asymmetric with respect to the two C–O groups of the ring [10–12], but to date there is no quantitative analysis of the spin-density distribution. Therefore, the average centre of spin density on Q_A^- cannot be determined. For reference, we give the distance to O5 on the Q_A. On the spin label, the spin density is almost equally distributed over the N and O atoms of the nitroxide group, making the geometric centre of N and O a good approximation for the average centre of spin density.

The distance between Q_A and the nitroxide group of the spin label further depends on the conformation of the linker joining the spin-label ring to the protein backbone atoms. From the X-ray structure, only the location of the atoms of the cysteine to which the spin label is attached, i.e., the C_α and C_β atoms can be obtained. The length of the tether in the extended conformation is 0.56 nm, measured from the C_β atom of the protein to the nitroxide

group. Therefore, the distance from the nitroxide group to Q_A can differ substantially from the distance between the C_β atom of the cysteine and Q_A.

Previously, this factor was taken into account [13], suggesting that by comparing the distance from C_α and C_β to the centre of interest, the orientation of the spin label can be estimated: If the distance from the centre of interest to C_α is shorter than the distance to C_β the spin label must point away from C_β, thus the distance from the centre of interest to the spin label is larger than the distance to C_β, whereas in the opposite case the distance is smaller. For H156, the distance between O5 of Q_A and C_α (3.15 nm) is a little larger than that of C_β (3.06 nm), suggesting that the nitroxide of the spin label points towards Q_A and that the distance between C_β and Q_A should be an upper limit for the distance from the nitroxide group to Q_A. The experimentally determined distance is 3.05 nm, thus in agreement with that approach. The remaining centres of spin density on Q_A are closer to C_α and C_β of H156, thus, with respect to these centres, the measured distance is larger than what is expected from the model.

The width of the distance distribution is 0.24 nm. For the interaction of the spin label with a native cofactor that is firmly anchored in the protein, the only source of a broadening of the distance distribution are multiple conformations of the spin label with respect to the protein backbone. Thus, in the case of spin-label-cofactor interactions the width of the distance distribution should be smaller than for the interaction of two spin labels with each other. The analysis of Freed et al. [13] suggests that a single spin label can have a conformational distribution between 0.2 and 0.6 nm. Thus, the width observed is consistent with the width expected for a single spin label.

Given the relatively large ambiguity of the position of the spin label due to the conformation of the spin-label linker, the distances cannot be interpreted based on the X-ray structure alone. Therefore, the orientation of the linker attaching the spin label to the protein backbone was determined by MD calculations on the entire protein. This yields the position of the nitroxide group of the spin label, and thus allows to determine the distance. The conformational space visited by the spin label during the MD run determines the width of the distance distribution, which is compared to the experimental one.

For the distance from O5 of Q_A to the centre of the N–O-bond, the MD simulations yield a distance distribution with an approximately Gaussian shape at 2.80 nm with a width of 0.17 nm (see Fig. 4B). The small width of the distribution derives from the fact that the linker conformation is restricted by a protein loop in the vicinity of the nitroxide. This finding agrees with the relatively low mobility of the spin label found by liquid-solution EPR [25]. The average distance is smaller than the distance between C_β of H156 and Q_A, which is in agreement with the model proposed by Freed et al. [13].

Energy minimization was performed for random structures visited during the MD run. This should model the situation in the frozen sample, where the orientations of the spin label populated at room temperature are frozen-in and form the ensemble of structures that is observed in the low-temperature experiment. The centre of the histogram of the distance distribution obtained by energy minimization (Fig. 4B) is close to the distribution from the MD run. The histogram is more asymmetric and wider than the distribution of the MD run. To quantify this, the histogram was fit to a Gaussian shape with the parameters given in Table 1. Apparently, as modelled in the MD simulations, the room-temperature conformations of the spin label and the ensemble of conformations in the low temperature sample do not have identical distance distributions, but the number of energy minimized structures is too small to unambiguously determine that point.

To compare the results of the MD simulations with the experimental ones, in Fig. 3C, the distance distribution of the MD run is compared to the distribution obtained from the DEER experiments. The width and the shape of the simulation agree well with the experiment, showing that the spread in the conformations of the spin-label linker is adequately modelled in the MD calculations. The average distance of 2.8 nm from the atom O5 of Q_A to the centre of the NO-group of the spin label in the MD simulations is significantly smaller than the distance obtained from experiment. The disagreement must be even larger, since the other centres of spin density on Q_A^- are closer to the nitroxide than O5 (see Table 2). For example, the smallest distance, 2.45 nm, is found for O2, which certainly also carries a large spin density. A quantitative analysis of this factor will only be possible once the assignment of spin densities over Q_A^- is known. To estimate how large the difference could be, we take the spin-density distribution of Q_A^- derived from DFT calculations in [14]. According to these calculations, the spin density on the C–O groups is 70% and slightly asymmetric. Using these spin densities yields an average distance of 2.62 nm for the structure given in Table 2. A symmetric spin density distribution only changes this distance by 0.01 nm, showing that small changes of the spin-density distribution have only minor effects on the distance.

Several factors could account for the discrepancy between the distance in the MD simulations and the experiment: (i) Incomplete sampling of the spin-label conformations, (ii) the charge on Q_A, that is present in the DEER experiment, but not in the X-ray structure or the MD simulations could play a role, (iii) the structure of the RC in frozen solution could differ from that in the crystal, and (iv) the structure could differ because the native Fe(II) is replaced by Zn(II).

Incomplete sampling of the spin-label conformations (i) should not be a problem, because the mobility of the spin label observed in liquid-solution, room-temperature EPR [25] is well represented in MD simulations using the same approach. Nevertheless, freezing of the sample could affect

the spin-label conformation and result in a different distance distribution than calculated from the MD run. The distance distribution after energy minimization (histogram) points in that direction, but there are not enough data points to unambiguously determine that. Assuming that the linker conformation is properly represented in the MD simulations, the discrepancy of the distances must be largely due to the protein backbone conformation in the X-ray structure, which is the starting point of the MD simulation.

It is difficult to envisage how the charge on Q_A^- (ii) could have a structural effect on the protein over such a long distance. Nevertheless, in principle, this point could be addressed by MD methods, provided that the run is long enough to allow relaxation of the protein backbone.

Differences in the structure of the RC in frozen solution and in the crystal (iii) could, for example, be due to the glycerol added to the frozen solution, which is absent in the crystal. There are suggestions that glycerol could affect the structure or the position of the H-subunit (Borovykh et al., unpublished). As the spin label is attached to the H-subunit, this could have an effect on the distance observed by DEER. Crystallization of the spin-labelled protein and EPR distance determination in the crystal would yield information about (iii). Given the challenges involved in the crystallization of membrane proteins this is an ambitious project. (iv) Previous experiments have not given indications for gross structural changes upon replacing the native Fe(II) by Zn(II). For example, electron-transfer rates between the cofactors did show significant differences in Fe(II) or Zn(II) RCs [15]. Nevertheless, a change in position of the H-subunit would not necessarily have an effect on the electron-transfer rates, and, therefore, could have escaped detection in the past. Thus, (iii) and (iv) are the most probable sources for the discrepancy between the distances observed by DEER and in the MD simulations. Further information about the origin of the discrepancy could be obtained by measuring the distance between Q_A^- and spin labels at other positions in the RC. Since the remaining native cystines in the RC are either too buried in the protein or in the detergent micelle to be accessible for labelling [25] this would require site-directed mutagenesis to introduce new spin-label sites. In the present study, we show that by our DEER approach, distances in such samples can be measured to high precision. This is the prerequisite to embark on the site-directed mutagenesis approach to this system.

3.1. Summary and outlook

We show that the distance between a cofactor and a spin label in an electron-transfer protein can be measured with a precision of ± 0.05 nm. To estimate if that would be sufficient to determine structural changes in a protein due to an electron-transfer reaction, we compare the crystallographic structures of the RC in the dark (charge-neutral) state (PDB-entry: AIJ) and in the charge-separated state (PDB-entry AIG), in which the primary electron donor D is oxidized (D^+) and the secondary quinone, Q_B, is reduced (Q_B^-) [2]. The distance between the C_β atom of H156 and O5 of Q_A in the charge separated state differs by 0.2 nm from that in the dark state. The precision of our method is sufficient to detect that change, confirming that the method is suitable to detect changes in protein conformation upon electron transfer.

4. Materials and methods

Reaction centres (RCs) of *Rb. sphaeroides* R26 were isolated according to Feher et al. [16]. For the pulsed EPR measurements, the native Fe(II)-ion ($S = 2$) was replaced with Zn(II) (ZnRCs) as described by Tiede and Dutton [17]. ZnRCs were solubilized in TEL-buffer consisting of 10 mM Tris–HCl (pH 8.0), 1 mM EDTA, and 0.025% lauryldimethylamine *N*-oxide. Labelling was done by adding the spin label 1-oxyl-2,2,5,5-tetramethyl-Δ-pyrroline-3-methyl methanethiosulfonate (MTSL - Toronto Research Chemicals Inc. (Canada)) in acetone to a solution of the RCs. The acetone concentration during the labelling was below 10% (v/v), see for details [25]. Spin-labelled ZnRCs are referred to as SL-ZnRCs. The ratio of bound spin label/RC was determined by cw-EPR to be 0.9 ± 0.2 [25]. The Q_A^- radical was generated by freezing the sample under illumination in the presence of a 10–30 times molar excess of sodium ascorbate (light sample). As a reference, a sample of the same batch of spin labelled ZnRCs that was kept in the dark was used (dark sample). For low temperature measurements 66% (v/v) of glycerol was added to the sample to provide a transparent glass when freezing. The final concentration of RCs was $A^{800} = 30\ \mathrm{cm}^{-1}$, i.e., approximately 100 μM.

4.1. EPR experiments

The EPR experiments were performed on a Bruker Elexsys E680 spectrometer (BrukerBiospin, Rheinstetten). The cw-EPR spectra were obtained at 40 K, using a rectangular cavity equipped with a Helium flow cryostat, model ESR 900 H. The electron-spin-echo detected EPR spectra were obtained in a dielectric resonator ER 4118 X-MD-5-W1 (BrukerBiospin, Rheinstetten) using a $p_{\pi/2}$–τ–p_π echo sequence. The cw- and electron-spin echo (ese)-detected EPR spectra were simulated with Matlab® using the Easyspin routines [18,19]. To account for the superposition of the signals of the spin label and Q_A^-, the simulated spectrum of Q_A^- was added to the spin-label spectrum, adjusting the intensity of the Q_A^- spectrum to give the best agreement with the experimental spectrum.

4.2. DEER experiments

For DEER experiments, the spectrometer was modified as described before [20]. The DEER experiment was per-

formed at 60 K using a Helium flow system by Oxford, model CF 935. The four-pulse DEER sequence [21] p_1–t_1–p_2–t_2–p_3 with a pump pulse inserted after p_2 was employed. Pulse lengths were 32 ns for p_1, p_2, and p_3, and amplitudes were adjusted to obtain a $\pi/2$ pulse for p_1 and π-pulses for p_2 and p_3. The pump-pulse length was 36 ns, and the pump power was adjusted for maximum inversion of the echo. Delay times were $t_1 = 200$ ns, $t_2 = 2000$ ns and the time T, at which the pump pulse was inserted after p_2 was varied. The observer field was set to the low field edge of the spin-label EPR spectrum and the pump frequency adjusted to coincide with the maximum of the ese-EPR spectrum, where the Q_A^--EPR signal is superimposed on the spin-label signal.

4.3. Analysis of DEER results

For the analysis of the distance distributions, firstly, Gaussian distance distributions were tried using the program DEERfit [5–7]. The parameters were adjusted manually, and errors were estimated by determining the magnitude of the changes in the parameters that resulted in simulated curves outside the noise limit of the experiment. For the fitting procedure with arbitrary distance distributions, the methods provided in the program DeerAnalysis2004 [5–7] were used. In all cases, a distance of approximately 3 nm was dominant. An additional smaller contribution at distances larger than 4 nm was always present, with a larger width of the distribution and a stronger deviation from Gaussian than that at the distance of approximately 3 nm. The distribution discussed in the text was obtained using Tikhonov regularization in the frequency domain.

4.4. Molecular dynamics

The initial structure was the high-resolution X-ray structure, 1AIJ (resolution 2.2 Å, dark state). The spin label was attached to position H156 [3,25]. The MD simulations of the protein in vacuum were performed as described earlier, using the Gromacs simulations suite [22–24]. The starting orientation of the spin label was such that the nitroxide head group was oriented towards the Fe(II) ion that is located between Q_A and Q_B. The dihedral angles of the spin-label linker were adjusted to avoid close contacts with the neighbouring side chains. Then the structure was energy minimized using steepest-descent and conjugate-gradient algorithms in 1000 steps. This involved a preparation run of 1 ns at 300 K with constraints on all-bonds and no position restraints. During this preparation run the average deviation of all C_α positions from their initial values converges within the first 400 ps to 0.12 nm. After this time the system was observed to be stable. The maximum value of the root mean square deviation of averaged C_α positions from their initial (crystal) positions is less than 0.18 nm. This shows that the absence of crystal contacts or the lack of the stabilizing effects of a lipid bilayer during the MD simulation does not lead to gross structural changes of the protein. Next, the temperature was gradually raised from 300 to 600 K, while the positions of the carbon, oxygen and nitrogen atoms of the backbone and the positions of the cofactors were restrained to avoid possible initial steps of unfolding of the protein. The system was equilibrated for 1 ns at 600 K. The resulting structure was used as the starting point for the MD run, which lasted 6 ns with time steps of 2 fs.

To better represent the experiments carried out at 60 K, 30 structures were chosen at arbitrary time points of the MD run and used as starting structures for energy minimization. This should simulate the freezing-in of different conformations in the low-temperature experiment. Thus, an ensemble of structures was generated. The distances observed in this ensemble of structures were compared to those of the MD run.

Acknowledgments

The work was performed under the auspices of the BIOMAC research school of Leiden University. The work would not have been possible without the continuous support of Edgar Groenen. Tatiana Shkuropatova is acknowledged for her help with the sample preparations. Financial support from the Volkswagen-Stiftung (Grant No. I/77587) and from the Dutch Science Organization (NWO/CW Grant No. 700-50-026) is gratefully acknowledged.

References

[1] D. Kleinfeld, M.Y. Okamura, G. Feher, Electron-transfer kinetics in photosynthetic reaction centers cooled to cryogenic temperatures in the charge-separated state—evidence for light-induced structural-changes, Biochemistry 23 (1984) 5780–5786.
[2] M.H.B. Stowell, T.M. McPhillips, D.C. Rees, S.M. Soltis, E. Abresch, G. Feher, Light-induced structural changes in photosynthetic reaction center: implications for mechanism of electron–proton transfer, Science 276 (1997) 812–816.
[3] O.G. Poluektov, L.M. Utschig, S. Dalosto, M.C. Thurnauer, Probing local dynamics of the photosynthetic bacterial reaction center with a cysteine specific spin label, J. Phys. Chem. B 107 (2003) 6239–6244.
[4] K. Sale, L.K. Song, Y.S. Liu, E. Perozo, P. Fajer, Explicit treatment of spin labels in modeling of distance constraints from dipolar EPR and DEER, J. Am. Chem. Soc. 127 (2005) 9334–9335.
[5] G. Jeschke, A. Koch, U. Jonas, A. Godt, Direct conversion of EPR dipolar time evolution data to distance distributions, J. Magn. Reson. 155 (2002) 72–82.
[6] G. Jeschke, Distance measurements in the nanometer range by pulse EPR, Chemphyschem 3 (2002) 927–932.
[7] G. Jeschke, Determination of the nanostructure of polymer materials by electron paramagnetic resonance spectroscopy, Macromol. Rapid Commun. 23 (2002) 227–246.
[8] G. Jeschke, G. Panek, A. Godt, A. Bender, H. Paulsen, Data analysis procedures for pulse ELDOR measurements of broad distance distributions, Appl. Magn. Reson. 26 (2004) 223–244.
[9] G. Jeschke, A. Bender, H. Paulsen, H. Zimmermann, A. Godt, Sensitivity enhancement in pulse EPR distance measurements, J. Magn. Reson. 169 (2004) 1–12.
[10] W. Lubitz, G. Feher, The primary and secondary accepters in bacterial photosynthesis III. Characterization of the quinone radicals

QA(-)center dot and QB(-center dot) by EPR and ENDOR, Appl. Magn. Reson. 17 (1999) 1–48.
[11] M. Rohrer, F. MacMillan, T.F. Prisner, A.T. Gardiner, K. Möbius, W. Lubitz, Pulsed ENDOR at 95 GHz on the primary acceptor ubisemiquinone Q(A)(-center dot) in photosynthetic bacterial reaction centers and related model systems, J. Phys. Chem. B 102 (1998) 4648–4657.
[12] J.S. van den Brink, A.P. Spoyalov, P. Gast, W.B.S. van Liemt, J. Raap, J. Lugtenburg, A.J. Hoff, Asymmetric binding of the primary acceptor quinone in reaction centers of the photosynthetic bacterium *Rhodobacter sphaeroides* R26, probed with Q-band (35 Ghz) Epr spectroscopy, FEBS Lett. 353 (1994) 273–276.
[13] P.P. Borbat, H.S. Mchaourab, J.H. Freed, Protein structure determination using long-distance constraints from double-quantum coherence ESR: study of T4 lysozyme, J. Am. Chem. Soc. 124 (2002) 5304–5314.
[14] P.J. O'Malley, The origin of the spin density asymmetry at the Q(A) binding site of type II photosynthetic reaction centres, Chem. Phys. Lett. 379 (2003) 277–281.
[15] C. Kirmaier, D. Holten, R.J. Debus, G. Feher, M.Y. Okamura, Primary photochemistry of iron-depleted and zinc-reconstituted reaction centers from rhodopseudomonas-sphaeroides, Proc. Natl. Acad. Sci. USA 83 (1986) 6407–6411.
[16] G. Feher, M.Y. Okamura, Chemical composition and properties of reaction centers, in: R.K. Clayton, W.R. Sistrom (Eds.), The Photosynthetic Bacteria, Plenum Press, New York, 1978, pp. 349–386.
[17] D.M. Tiede, P.L. Dutton, Orientation of the primary quinone of bacterial photosynthetic reaction centers contained in chromatophore and reconstituted membranes/ion centers contained in chromatophore and reconstituted membranes, Biochim. Biophys. Acta 637 (1981) 278–290.
[18] S. Stoll, PhD-thesis, ETH Zürich (2003).
[19] S. Stoll, A. Schweiger, EasySpin, a comprehensive software package for spectral simulation and analysis in EPR, J. Magn. Reson. 178 (2006) 42–55.
[20] I.M.C. van Amsterdam, M. Ubbink, G.W. Canters, M. Huber, Measurement of a Cu–Cu distance of 26 Å by a pulsed EPR method, Angewandte Chemie-International Edition 42 (2003) 62–64.
[21] M. Pannier, S. Veit, A. Godt, G. Jeschke, H.W. Spiess, Dead-time free measurement of dipole–dipole interactions between electron spins, J. Magn. Reson. 142 (2000) 331–340.
[22] H.J. Steinhoff, W.L. Hubbell, Calculation of electron paramagnetic resonance spectra from Brownian dynamics trajectories: application to nitroxide side chains in proteins, Biophys. J. 71 (1996) 2201–2212.
[23] H.J. Steinhoff, M. Müller, C. Beier, M. Pfeiffer, Molecular dynamics simulation and EPR spectroscopy of nitroxide side chains in bacteriorhodopsin, J. Mol. Liquids 84 (2000) 17–27.
[24] E. Lindahl, B. Hess, D. van der Spoel, GROMACS 3.0: a package for molecular simulation and trajectory analysis, J. Mol. Model. 7 (2001) 306–317.
[25] P. Gajula, I.V. Borovykh, C. Beier, P. Gast, T. Shkuropatova, H.-J. Steinhoff, Study of the structure and dynamics of spin-labeled photosynthetic reaction centers from *Rhodobacter sphaeroides* by electron paramagnetic resonance spectroscopy and molecular dynamics simulations, Appl. Magn. Reson. (submitted for publication).